THE JOURNAL OF BIOLOGICAL CHEMISTRY
Vol. 277, No. 18, Issue of May 3, pp. 16257–16264, 2002
© 2002 by The American Society for Biochemistry and Molecular Biology, Inc.
Printed in U.S.A.

Mycobacterium tuberculosis RecA Intein Possesses a Novel ATP-dependent Site-specific Double-stranded DNA Endonuclease Activity*

Received for publication, December 26, 2001, and in revised form, February 13, 2002
Published, JBC Papers in Press, February 15, 2002, DOI 10.1074/jbc.M112365200

N. Guhan‡ and K. Muniyappa§

From the Department of Biochemistry, Indian Institute of Science, Bangalore 560 012, India

Mycobacterium tuberculosis recA **harbors an intervening sequence in its open reading frame, presumed to encode an endonuclease (PI-*Mtu*I) required for intein homing in inteinless *recA* allele. Although the protein-splicing ability of PI-*Mtu*I has been characterized, the identification of its putative endonuclease activity has remained elusive. To investigate whether PI-*Mtu*I possesses endonuclease activity, *recA* intervening sequence was cloned, overexpressed, and purified to homogeneity. Here we show that PI-*Mtu*I bound both single- and double-stranded DNA with similar affinity but failed to cleave DNA in the absence of cofactors. Significantly, PI-*Mtu*I nicked supercoiled DNA in the presence of alternative cofactors but required both Mn^{2+} and ATP to generate linear double-stranded DNA. We observed that PI-*Mtu*I was able to inflict a staggered double-strand break 24 bp upstream of the insertion site in the inteinless *recA* allele. Similar to a few homing endonucleases, DNA cleavage by PI-*Mtu*I was specific with an exceptionally long cleavage site spanning 22 bp. The kinetic mechanism of PI-*Mtu*I promoted cleavage supports a sequential rather than concerted pathway of strand cleavage with the formation of nicked double-stranded DNA as an intermediate. Together, these results reveal that RecA intein is a novel Mn^{2+}-ATP-dependent double-strand specific endonuclease, which is likely to be important for homing process *in vivo*.**

The prototype *Escherichia coli* RecA protein plays a central role in homologous recombination, DNA repair, restoration of stalled replication forks and SOS response (reviewed in Refs. 1–4). The process of homologous recombination, which is the main mechanism of genetic exchange and RecA, a ubiquitous multifunctional protein, is substantially conserved among a range of organisms (reviewed in Ref. 5). In contrast, the *recA* of *Mycobacterium tuberculosis* and *Mycobacterium leprae* contain an in-frame insertion of an intein-coding sequence (6, 7). Following the synthesis of RecA precursor, an internal domain, termed the intein, is excised from the precursor and the two flanking domains called exteins are ligated together to generate functionally active RecA protein (8). Previously, we have reported the recombination-like activities and x-ray structure of the spliced form of *M. tuberculosis* RecA protein (9–11). However, the biochemical function of *M. tuberculosis* RecA intein and its possible role in homologous recombination promoted by its cognate RecA remains obscure.

Inteins are protein-splicing elements that contain conserved domains with sequence homology to a diverse family of homing endonucleases (reviewed in Refs. 12–16). The hallmark of homing endonucleases, like restriction enzymes, is their ability to cleave double-stranded DNA at specific target sites (12, 17). First identified in a mobile group I intron of yeast mitochondria (18, 19); genes for homing endonucleases have since been found in group II introns and intein-coding sequences of unicellular eukaryotes, archaea, and eubacteria (12). On the basis of conserved motifs, these enzymes fall into four classes: (*a*) LAGLIDADG, (*b*) GIY-YIG, (*c*) H-N-H, and (*d*) His-Cys box or zinc finger enzymes (12, 16, 20). The LAGLIDADG class is the largest, more widespread with >200 known members, each containing one or two copies of the dodecapeptide motif. These enzymes are highly specific, with very long, rare recognition sites that span intein integration sites in homologous alleles that lack the intron or intein-coding sequence. Biochemical and structural studies have demonstrated that homing endonucleases composed of a single copy of LAGLIDADG motif function as homodimers, whereas double-motif enzymes act as monomers. The catalytic centers carry two essential aspartate residues in the LAGLIDADG motif. These residues function by coordinating a divalent cation necessary for catalysis, Mg^{2+} being the preferred metal ion (12–16).

It is clear from the scrutiny of complete genome sequence of *M. tuberculosis* that, in addition to *recA* (6, 7), as defined by both *in vivo* and *in vitro* studies, intein-coding sequences are embedded in the open reading frames of *dnaA* and *Rv1461* (21). The deduced amino acid sequence of *M. tuberculosis recA* intervening sequence disclosed the existence of two copies of LAGLIDADG motifs. The protein-splicing ability of PI-*Mtu*I[1] has been studied extensively (22–25); however, the endonuclease activity has not been demonstrated. To this end, PI-*Mtu*I was cloned, overexpressed, and purified, to explore its biochemical functions. Significantly, the results presented here reveal that RecA intein is a novel Mn^{2+}-ATP-dependent, double-strand-specific endonuclease, which is likely to be important for intein homing *in vivo*.

MATERIALS AND METHODS

All the chemicals used in this study are of analytical grade. Buffers were prepared using deionized water. Restriction enzymes, Nylon N^+

* This work was supported in part by grants from the Wellcome Trust, UK, and Indian Council of Medical Research, New Delhi, India. The costs of publication of this article were defrayed in part by the payment of page charges. This article must therefore be hereby marked "*advertisement*" in accordance with 18 U.S.C. Section 1734 solely to indicate this fact.

‡ Supported by a fellowship from the Council of Scientific and Industrial Research, New Delhi, India.

§ To whom correspondence should be addressed. Tel.: 91-80-360-0278; Fax: 91-80-360-0814; E-mail: kmbc@biochem.iisc.ernet.in.

[1] The abbreviations used are: PI-*Mtu*I, RecA intein endonuclease of *M. tuberculosis*; ATPγS, adenosine 5′-*O*-(thiotriphosphate); DTT, dithiothreitol; form I DNA, negatively supercoiled DNA; form II DNA, nicked circular double-stranded DNA, form III DNA, linear double-stranded DNA; SPR, surface plasmon resonance; ssDNA, single-stranded DNA; GST, glutathione *S*-transferase.

Downloaded from www.jbc.org by guest, on November 18, 2010

membrane, Sephacryl S-200 were purchased from Amersham Biosciences, Inc., Asia Pacific Pvt. Ltd, Hong Kong. Phage T4 polynucleotide kinase was purchased from Invitrogen, New York, NY. Hydroxyapatite was obtained from Bio-Rad Laboratories, Hercules, CA. Circular single-stranded and negatively supercoiled plasmid pEJ244 DNA were prepared by sucrose density gradient centrifugation as described previously (26). The DNA was dissolved in 10 mM Tris-HCl buffer (pH 7.5) containing 1 mM EDTA, and the concentrations are expressed in moles of nucleotide residues.

Construction of PI-MtuI-GST Fusion Plasmid—Plasmid pEJ135 (kindly provided by E. O. Davis and M. J. Colston, National Institutes for Medical Research, London) bearing *M. tuberculosis recA* gene was digested with *Kpn*I and *Hin*dIII. The 1.6-kb DNA fragment purified from agarose gel was incubated with T4 DNA polymerase (27). The *Kpn*I-*Hin*dIII fragment contained the RecA intein coding sequence and a portion of *recA* corresponding to 15 amino acid residues of N-extein and 75 amino acid residues of C-extein flanking the intein autoproteolytic cleavage sites. The fragment was subcloned into expression vector pGEX-2T at the *Sma*I site. The recombinant plasmid was referred to as pGRI. The plasmid contains in-frame fusion of the RecA intein-coding sequence with GST. DNA sequence of the insert was determined using the automated ABI Prism DNA sequencer (PerkinElmer Life Sciences) to confirm the sequence. The recombinant plasmid was transformed and amplified in *E. coli* strain DH5α.

Expression and Purification of PI-MtuI Endonuclease—Optimal expression of PI-*Mtu*I was obtained in *E. coli* strain DH5α by growth at 37 °C in LB broth until A_{600} = 0.4, followed by addition of isopropyl-1-thio-β-D-galactopyranoside to a final concentration of 0.5 mM. Cells were further incubated for 4 h and harvested later by centrifugation at 5000 × *g* for 10 min and stored at −70 °C. All subsequent steps were performed at 4 °C unless otherwise stated. Cells (30 g) were resuspended in buffer A (50 mM Tris-HCl, pH 8.0, 10% sucrose) and incubated with 20 mg of lysozyme on ice for 30 min. Cells were lysed by sonication (Vibra cell sonicator, Sonics and Material Inc., Danbury, CT) at setting 9 and 60% duty cycles in a pulse mode for 15 min. The supernatant was obtained by centrifugation at 30,000 rpm for 1 h in a Ti-45 Beckman rotor. Polyethyleneimine acetate (pH 6.5) was added to the supernatant to a final concentration of 0.2% over a period of 15 min with constant stirring. Precipitates were recovered by centrifugation at 12,000 rpm for 15 min. To the supernatant, $(NH_4)_2SO_4$ was added to a final concentration of 0.3 g/ml with continuous stirring over a period of 1 h. The suspension was centrifuged at 15,000 rpm for 15 min, and the pellet was resuspended in buffer B (20 mM sodium phosphate, pH 6.5, 10% glycerol, 0.1 mM EDTA, 5 mM 2-mercaptoethanol). Protein solution was dialyzed against 1 liter of buffer B with three changes over 18 h. The dialysate was centrifuged at 15,000 rpm for 15 min, and the supernatant was loaded onto a hydroxyapatite column (2 × 11 cm), which had been equilibrated with buffer B. The column was washed with buffer B until the eluate contained no material that absorbed light at 280 nm. The bound proteins were eluted with a linear gradient of 20 to 250 mM sodium phosphate in buffer B. Fractions containing PI-*Mtu*I (ascertained by immunoblot assay using antibodies raised against *M. tuberculosis* RecA precursor) were pooled and precipitated by the addition of $(NH_4)_2SO_4$ to a final concentration of 0.3 g/ml. The precipitate was collected by centrifugation as described above and resuspended in buffer C (20 mM Tris acetate, pH 7.5, 1 M NaCl, 5 mM 2-mercaptoethanol, 0.1 mM EDTA, 10% glycerol), loaded onto a Sephacryl S 200 column (1.7 × 105 cm), which had been equilibrated with buffer C. The fractions containing PI-*Mtu*I were combined, precipitated with $(NH_4)_2SO_4$, and dialyzed against buffer C and loaded onto a Superdex 200 column (26 × 60 cm) (Amersham Biosciences, Inc.). Peak fractions containing PI-*Mtu*I were pooled, dialyzed against storage buffer (20 mM Tris-HCl, pH 7.5, 100 mM NaCl, 1 mM DTT, 50% glycerol). Aliquots of the dialysate were stored at −20 °C. The final yield of PI-*Mtu*I was in the range of 2.5 mg/liter of culture. Protein purity was ascertained by 10% SDS-PAGE/Coomassie Blue staining and was generally >98% pure. The concentration of protein was determined by dye binding method using bovine serum albumin as the standard (28) and expressed in moles of monomers per liter. PI-*Mtu*I stored in 50% glycerol at −20 °C was stable for 6 months.

Electrophoretic Mobility Shift Assay—Reaction mixtures (10 μl) contained 25 mM Tris-HCl (pH 7.5), 0.4 mM DTT, 3 μM ^{32}P-labeled 75-mer DNA containing the PI-*Mtu*I cleavage site (underlined sequence) 5′-dACGCTCAAGGACGGTACCAACGCGGTCGGCAACCGCACCCGGGTCAAGGTCGTCAAGAACAAGTGTTCGCCCCCC-3′ or 75-bp DNA (75-mer DNA annealed to its complementary strand) with increasing concentrations of PI-*Mtu*I. After incubation at 37 °C for 10 min, the reactions were terminated by the addition of 1 μl of loading buffer (20% glycerol containing 0.12% (w/v) each of bromphenol blue and xylene cyanol) to each reaction mixture. Samples were separated on an 8% polyacrylamide gel by electrophoresis in 40 mM Tris acetate buffer (pH 7.5) containing 0.1 mM EDTA at 12 V/cm for 5 h at 4 °C. The gel was dried on a Whatman 3MM filter paper and visualized by autoradiography.

DNA Binding and Kinetic Studies—Surface plasmon resonance (SPR) measurements were performed using BIAcore 2000 system with streptavidin-coated sensor chips. All procedures were automated by using repetitive cycles of sample injection, washing, and regeneration. The chip contained streptavidin covalently immobilized on a carboxymethylated dextran layer at the surface. The DNA surface was prepared by immobilizing a biotinylated 60-mer DNA (5′-dAATTCTGGGTGTGTGGGTGTGTGGGTGTGGTCAAGTTGACTACGTATACATC-Biotin-3′) or 27-bp DNA (5′-Biotin-dTCGAGATCAAGGTCAAAGGTCACTCGC-3′ annealed to its complementary strand) according to manufacturer's instructions. The chips produced response signals of ~400 response units. An empty flow cell served as a control. PI-*Mtu*I was diluted in binding buffer containing 25 mM Tris-HCl (pH 7.5), 100 mM NaCl, 0.4 mM DTT, and 0.1 mM EDTA. Solutions containing increasing concentrations of PI-*Mtu*I, designated as the "analyte," was injected onto the biosensor chip for 10 min at a flow rate of 5 μl/min for association, followed by a 5-min buffer injection for dissociation. Under these conditions, nonspecific binding of PI-*Mtu*I to the control flow cell was insignificant. Specific binding in real-time and physical parameters of interaction was determined by analyzing the sensograms using the BIAcore evaluation software version 3.0. Specific SPR was plotted as function of time obtained at different analyte concentrations. The kinetic rate constants and the equilibrium binding constants were determined. After each injection, the surface was regenerated using 0.15% SDS, followed by buffer wash.

Endonuclease Assay—Reaction mixtures (25 μl) contained 25 mM Tris-HCl buffer (pH 7.5), 3 mM $MnCl_2$, 1.5 mM ATP, 0.4 mM DTT, and 16 μM of negatively supercoiled pEJ244 plasmid DNA. The concentration of PI-*Mtu*I in each reaction is given in the figure legends. Plasmid pEJ244 bears one intein-less *M. tuberculosis recA* allele [In$^-$:*recA*] cloned into pTZ18R. After appropriate time of incubation at 37 °C, the reaction was stopped by the addition of 0.1% SDS followed by deproteinization with proteinase K (0.2 mg/ml) for 15 min at 37 °C. To the samples, 3 μl of gel loading buffer was added. The samples were then separated by electrophoresis through 0.8% agarose gel at 3 V/cm in 89 mM Tris borate buffer (pH 8.3). The bands were visualized by staining with 0.5 μg/ml ethidium bromide. The gel was transferred to Nylon N$^+$ membrane and developed by Southern hybridization (27). Quantification of bands was performed by UVI-BandMap software and plotted using GraphPad Prism 2.0 (UVI-Tech gel documentation system).

Immunological Techniques—Antibodies to *M. tuberculosis* RecA precursor (9) and PI-*Mtu*I were prepared in rabbits and characterized using standard procedures. Protein samples were electrophoresed on SDS-PAGE, transferred to nitrocellulose membrane, and visualized by chemiluminescence method as described (29, 30). Immunodepletion assay was performed by incubation of preimmune IgG-Sepharose or anti-PI-*Mtu*I IgG-protein A-Sepharose with 20 μg of PI-*Mtu*I in the endonuclease assay buffer at 4 °C for 2 h with continuous stirring. The slurry was centrifuged at 6000 rpm at 4 °C for 2 min, and the supernatant was assayed for the presence of Mn^{2+}-ATP-dependent PI-*Mtu*I endonuclease as described above.

Mapping of the PI-MtuI Cleavage Sites in Target DNA—The DNA fragment containing the *recA* intein insertion site (inteinless *recA* allele) was generated from plasmid pEJ244 by digestion with *Sma*I and *Hin*fI. The fragment was 5′-labeled using [γ-^{32}P]ATP and polynucleotide kinase. The reaction products were separated by electrophoresis on 8%polyacrylamide gels in 89 mM Tris borate buffer (pH 8.3) containing 2 mM EDTA. The bands corresponding to 44- and 77-bp DNA were excised from the gel, ground into small pieces, eluted with 10 mM Tris-HCl buffer (pH 7.5) containing 1 mM EDTA, extracted with phenol:chloroform:isoamyl alcohol solution, and DNA was precipitated by ethanol. About 0.1 μM PI-*Mtu*I was incubated with ~100 ng of ^{32}P-labeled DNA in the presence of 1 mM ATP and 3 mM $MnCl_2$ in reaction conditions similar to those described above. The protein was digested with proteinase K (0.2 mg/ml) for 15 min at 37 °C. The reaction products were extracted with phenol:chloroform:isoamyl alcohol solution, and DNA was precipitated by ethanol. The pellets were dissolved in gel loading buffer (95% formamide, 10 mM NaOH, 0.2% bromophenol blue, and 0.2% xylene cyanol) and boiled for 10 min followed by immediate cooling to 4 °C. Aliquots of the sample was subjected to the Maxam-Gilbert chemical sequencing reaction, and electrophoresed through a 14% polyacrylamide gel in the presence of 8 M urea in 89 mM Tris borate

Downloaded from www.jbc.org by guest, on November 18, 2010

buffer (pH 8.3) at 1800 V for 3.5 h (31). The gel was dried onto a 3MM Whatman filter paper and exposed to a phosphorimaging screen for 3 h for visualization of the bands. Signals were quantified using an Image Gauge version 3.0 (Fuji Science Laboratory, Japan).

RESULTS

Expression and Purification of PI-MtuI Endonuclease from E. coli—A DNA fragment containing *M. tuberculosis recA* intein-coding sequence and a portion of *recA* gene corresponding to 15 and 75 amino acid residues from N- and C-exteins, respectively, flanking the intein autoproteolytic cleavage sites, was subcloned in-frame with GST in an expression vector, pGEX-2T. The resultant plasmid, pGRI, was transformed into *E. coli* strain DH5α, and expression of fusion protein was induced by the addition of isopropyl-1-thio-β-D-galactopyranoside. Soluble extracts from induced cells were used to ascertain expression of fusion protein by SDS-polyacrylamide gel electrophoresis, visualized by Coomassie Blue staining and immunoblot analysis with polyclonal antibodies directed against *M. tuberculosis* RecA precursor. A band corresponding to the predicted size of fusion protein (84 kDa) was not detectable in the induced cell lysates. In contrast, we observed two bands: one identical to the native size of *M. tuberculosis* RecA intein (48 kDa) as calculated from deduced amino acid sequence, and the second corresponding to the combined size of GST plus portions of N- and C-exteins of RecA (36 kDa) (Fig. 1*A*). Consistent with these results, an immunoreactive species corresponding to the size of the fusion protein was not detectable in cell lysates. However, we observed a slower migrating immunoreactive band of the size of PI-*Mtu*I-GST fusion protein in an enriched fraction, thereby confirming the synthesis of fusion protein (*lane 3*, Fig. 1*B*).

The soluble PI-*Mtu*I was purified to homogeneity by precipitation with polymin P, $(NH_4)_2SO_4$ fractionation, chromatography over hydroxyapatite and gel filtration on Superdex 200 column (Fig. 1*A*). Estimates of molecular mass for the intact protein based on SDS-PAGE and gel filtration on Superdex 75 column, suggested that PI-*Mtu*I is a 48-kDa species, consistent with deduced amino acid sequence. The identity of the expressed and purified PI-*Mtu*I was verified by sequencing 10 amino acid residues at the N-terminal end. The determined amino acid sequence was as follows: NH_2-CLAEGTRIFD-COO^-, identical to that predicted from the nucleotide sequence. The presence of cysteine at the N-terminal end indicated correct splicing of PI-*Mtu*I in *E. coli*. Purified PI-*Mtu*I was examined in an *in vitro* assay for the presence of exonuclease and was observed to be devoid of detectable 3′→5′ or 5′→3′ exonuclease activities.

Interaction of PI-MtuI with Single- and Double-stranded DNA—To investigate the ability of PI-*Mtu*I to bind DNA, we used electrophoretic mobility shift assay with substrates containing the PI-*Mtu*I cleavage site (see below). The formation of PI-*Mtu*I·DNA complexes was assayed by mobility shifts in polyacrylamide gels relative to free DNA and analyzed by autoradiography. As shown in Fig. 2, PI-*Mtu*I bound to single- and double-stranded DNA as indicated by the reduced mobility of the band corresponding to free DNA as increasing amounts of PI-*Mtu*I were added. However, the amount of PI-*Mtu*I required for incorporating >90% of DNA into protein·DNA complexes differed between single- and double-stranded DNA. A 2-fold higher amount of PI-*Mtu*I was required to achieve a comparable effect with single-stranded DNA. Similar results were also obtained with PI-*Mtu*I with DNA substrates lacking the cleavage site (data not shown). Varying the period of incubation prior to electrophoresis revealed that binding occurred maximally with briefest incubation times tested at 37 °C (data not shown).

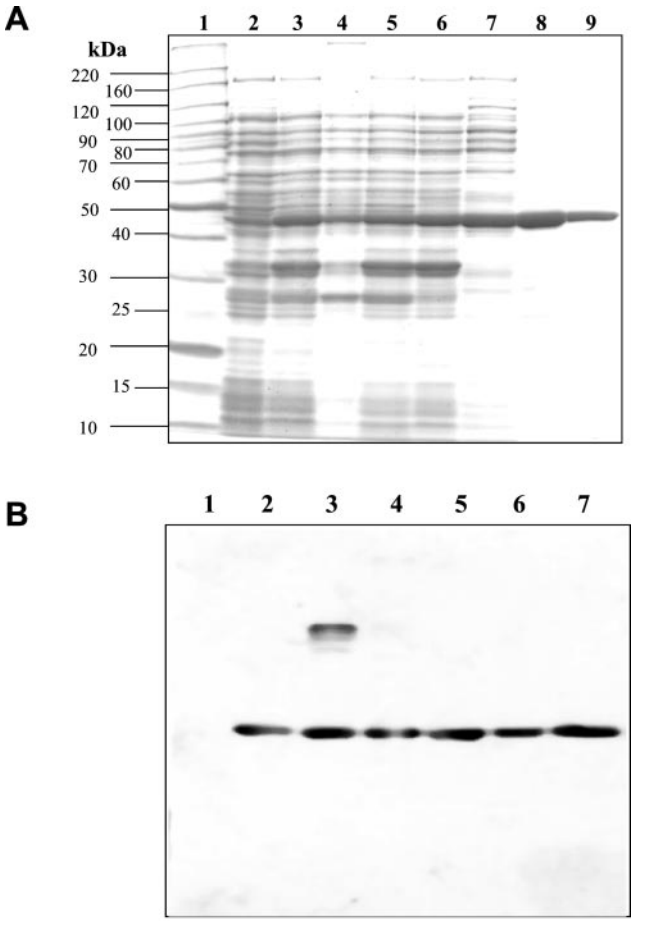

FIG. 1. **SDS-PAGE analysis showing induced expression of PI-*Mtu*I in *E. coli* and at various stages during its purification.** *A*, approximately 10 μg of protein was separated by SDS-PAGE and visualized by staining with Coomassie Blue. *Lanes*: *1*, molecular mass markers (Invitrogen); *2*, uninduced cell lysate; *3*, induced cell lysate; *4*, polymin P pellet fraction; *5*, polymin P supernatant fraction; *6*, $(NH_4)_2SO_4$ pellet fraction; *7*, hydroxyapatite eluate fraction; *8*, Sephacryl S 200 fraction; *9*, Superdex 200 gel filtration fraction. *B*, immunoblot analysis of PI-*Mtu*I. After SDS-PAGE as in *A*, the proteins were transferred to a nitrocellulose membrane, stained with anti-PI-*Mtu*I polyclonal antibodies, and visualized as described under "Materials and Methods." *Lanes*: *1*, uninduced cell lysate; *2*, induced cell lysate; *3*, polymin P pellet fraction; *4*, $(NH_4)_2SO_4$ pellet fraction; *5*, hydroxyapatite eluate fraction; *6*, Sephacryl S 200 fraction; *7*, Superdex 200 gel filtration fraction.

The kinetics of interaction of PI-*Mtu*I with DNA in real-time was monitored by SPR spectroscopy using DNA lacking the cleavage site. Under these conditions, binding of PI-*Mtu*I to DNA was independent of the presence of the cleavage site. Streptavidin sensor chip was derivatized with 60-mer DNA tagged with a 3′-terminal biotin, or 27-bp DNA bearing biotin at the 5′-end of the upper strand. The DNA on the chip was designated arbitrarily as the ligand, whereas a solution containing PI-*Mtu*I, designated as the "analyte" was passed over the sensor chip in a microfluidics chamber. To collect kinetic data, a range of concentrations of PI-*Mtu*I was injected over the immobilized DNA and reference surface for a period of 10 min. The chip was then washed with the binding buffer for additional 5-min. Specific binding of PI-*Mtu*I to single- or double-stranded DNA resulted in a substantial enhancement of mass in a concentration-dependent manner (data not shown). Specific binding of PI-*Mtu*I to the immobilized DNA was qualitatively detected by the increase in resonance units relative to control surface. Responses from the latter were used to correct for refractive index changes and instrument noise. A detailed

Downloaded from www.jbc.org by guest, on November 18, 2010

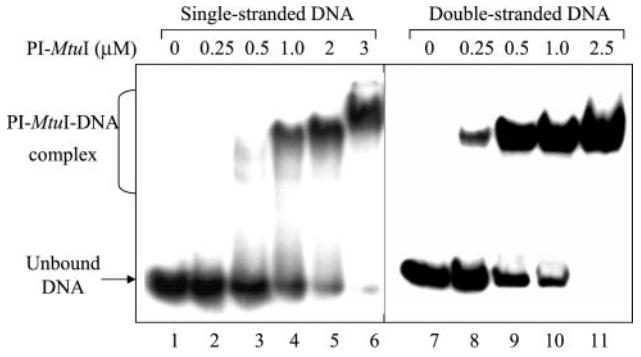

FIG. 2. **PI-*Mtu*I forms a stable binary complex with single- or double-stranded DNA.** Reaction mixtures containing 3 μM ^{32}P-labeled 75-mer or 75-bp DNA was mixed with increasing concentrations of PI-*Mtu*I in the absence of a metal ion and incubated as described under "Materials and Methods." *Lanes 1* and *7*, substrate DNA lacking PI-*Mtu*I. *Lanes 2–6*, 75-mer DNA with PI-*Mtu*I at concentration indicated on *top of each lane*; *lanes 8–11*, 75-bp DNA with PI-*Mtu*I at the concentrations indicated on *top of each lane*. The positions of unbound DNA and PI-*Mtu*I·DNA complexes are indicated on the *left*.

kinetic analysis was performed by globally fitting the association and dissociation phase data from each surface. This approach has provided quantitative estimates of binding affinities and on/off rates of reaction (Table I). The apparent equilibrium dissociation constant for both single- and double-stranded DNA was in the range of 28 nM. These K_d values are in the same range as reported for PI-*Pfu*I (13 nM) and PI-*Sce*I (3.7 nM) (32, 33). Also, these results suggest that PI-*Mtu*I could bind tightly to DNA in the absence of divalent cations, similar to PI-*Pfu*I or PI-*Sce*I (32, 33). Although our results are insufficient to allow determination of the stoichiometric ratio of binding of PI-*Mtu*I to DNA, following conclusions could be drawn. First, binding of PI-*Mtu*I to DNA does not require a target substrate containing the inteinless *recA* allele. Second, PI-*Mtu*I binds to single- and double-stranded DNA to a similar extent and, more importantly, is independent of topology, divalent metal ions and NTPs.

PI-MtuI Displays Endonuclease Activity—To test whether binding of PI-*Mtu*I to DNA ensues in endonuclease activity, we used negatively supercoiled (form I) pEJ244 DNA containing inteinless *recA* allele as the substrate. The site for insertion of *recA* intervening sequence occurs once in pEJ244 plasmid DNA. The rationale for using form I DNA (likely to be the *in vivo* target) rather than linear double-stranded DNA would be to permit detection of even nicking endonuclease activity of PI-*Mtu*I on supercoiled plasmids. Single-strand nicking would result in loss of negative supercoiling and, consequently, nicked circular duplex DNA (form II) could readily be distinguishable from that of form I DNA in a gel assay. Cleavage assays were performed by mixing PI-*Mtu*I with DNA in the presence of alternative divalent cations. After incubation, the reaction mixtures were deproteinized and the reaction products were separated by gel electrophoresis. The DNA substrate and cleaved products were visualized by staining with ethidium bromide, followed by Southern hybridization and autoradiography (Fig. 3). Although PI-*Mtu*I could interact with DNA in the absence of divalent cations (Fig. 2) but failed to cleave DNA (*lane 1*, Fig. 3). Significantly, PI-*Mtu*I displayed weak nicking endonuclease activity in the presence of a variety of cofactors resulting in the conversion of form I DNA to form II DNA (compare *lane 1* with *lanes 2–14*, Fig. 3). However, in the presence of ATP and $MnCl_2$, PI-*Mtu*I inflicted a double-strand break on form I DNA leading to the generation of form III DNA with no additional cleavages (*lane 8*, Fig. 3). To examine the role of ATP, we asked whether dATP in the presence of Mg^{2+} or Mn^{2+} could assist in the PI-*Mtu*I promoted double-stranded DNA cleavage. In parallel, we also tested whether ATP hydrolysis was required for the generation of form III DNA. In both cases, addition of dATP or ATPγS in the presence of either Mg^{2+} or Mn^{2+} abrogated the generation of form III DNA (*lanes 5*, *6*, *9*, and *10*, Fig. 3). Essentially, similar results were obtained with Mg^{2+}, Ca^{2+}, or Zn^{2+} alone or together with ATP. Thus, these results indicate that PI-*Mtu*I requires Mn^{2+}, and ATP hydrolysis for cleavage of double-stranded DNA.

Intriguingly, PI-*Mtu*I showed an unusual dependence for ATP. One factor that might account for the presence of Mn^{2+}-ATP-dependent endonuclease could be attributable to a contaminating endonuclease. The identity of PI-*Mtu*I was established by SDS-PAGE, and sequencing 10 amino acid residues at the N-terminal end. To seek further confirmation, immunodepletion assay was performed with anti-PI-*Mtu*I IgG-protein A-Sepharose or preimmune IgG-protein A-Sepharose. The resultant supernatant was assayed for Mn^{2+}-ATP-dependent endonuclease. Although the supernatant obtained from incubation with preimmune IgG displayed Mn^{2+}-ATP-dependent endonuclease activity, the same from anti-PI-*Mtu*I-treated sample lacked such an activity (data not shown). In addition, Mn^{2+}-ATP-dependent endonuclease cofractionated exactly with PI-*Mtu*I after Superdex 200 gel filtration. Together, these results argue that Mn^{2+}-ATP-dependent endonuclease activity is intrinsic to PI-*Mtu*I.

PI-MtuI Is Double-strand DNA-specific Endonuclease—Our experiments demonstrate that PI-*Mtu*I interacted with both single- and double-stranded DNA with similar affinity (Fig. 2 and Table I). The stable binding of PI-*Mtu*I to ssDNA indicated that it might ensue in nicking of single-stranded DNA. To seek functional relationship between binding and cleavage, a fixed amount of pEJ244 form I or ssDNA was mixed with increasing amounts of PI-*Mtu*I in the presence of Mn^{2+} and ATP as described above. Following incubation, reaction mixtures were deproteinized, and the resulting DNA was analyzed by agarose gel electrophoresis. The data in Fig. 4 indicate that PI-*Mtu*I cleaved form I but not ssDNA. These results establish the notion that PI-*Mtu*I is a double-stranded DNA-specific endonuclease.

Specific Requirements for PI-MtuI Endonuclease Activity—The parameters that influence the efficiency of endonuclease activity of PI-*Mtu*I were tested by monitoring the cleavage of pEJ244 form I DNA relative to Mn^{2+}, ATP, pH, and temperature conditions. We observed that both Mn^{2+} and ATP were essential to evoke double-stranded DNA cleavage activity of PI-*Mtu*I. Both cleavage and nicking of double-stranded DNA was maximal in a buffer containing 3 mM Mn^{2+} (Fig. 5*A*), 1.5 mM ATP (Fig. 5*B*), pH 7.5 (Fig. 5*C*), at 37 °C (Fig. 5*D*). Interestingly, we observed significant nicking endonuclease activity across a wide range of ATP concentrations. It is possible that the lack of corresponding increase in the formation of form III DNA may be due to changes in the concentration of ADP in the reaction mixture. However, the likely effect of ADP was excluded by performing the reactions under ATP regeneration conditions, which failed to increase the conversion of form II to form III DNA (data not shown).

We next examined the effect of added NaCl and potassium glutamate on the endonuclease activity of PI-*Mtu*I. A representative experiment performed in the presence of increasing concentrations of NaCl or potassium glutamate is shown in Fig. 6. Addition of 50 mM either NaCl (*lane 3*, Fig. 6) or potassium glutamate (*lane 10*, Fig. 6) reduced cleavage but not nicking activity of PI-*Mtu*I. However, further increase in ionic strength abolished double-strand cleavage activity (*lanes 4–9* and *11–16*, Fig. 6).

Kinetics and the Pathway of PI-MtuI Cleavage Reaction—We

Downloaded from www.jbc.org by guest, on November 18, 2010

TABLE I
Kinetic and steady-state parameters for the interaction of PI-MtuI with single- and double-stranded DNA

Analyte	Ligand	k_{on}	k_{off}	K_A	K_D
		$M^{-1}\ s^{-1}$	s^{-1}	M^{-1}	M
PI-*Mtu*I	60-mer DNA	1.81×10^5	5.02×10^{-3}	3.6×10^7	2.78×10^{-8}
	27-bp DNA	8.89×10^4	2.41×10^{-3}	3.69×10^7	2.71×10^{-8}

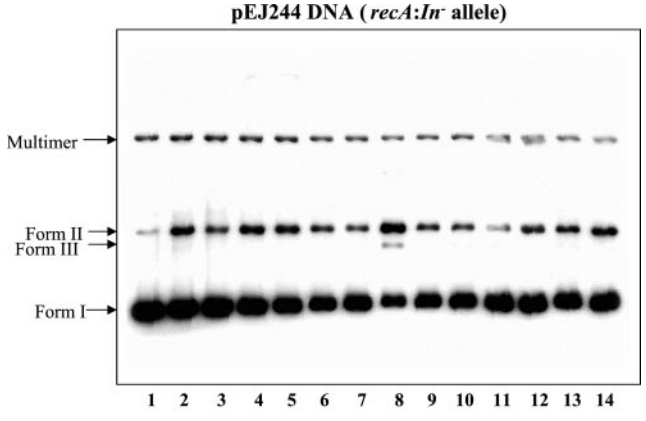

FIG. 3. **Identification of endonuclease activity of PI-*Mtu*I on cognate substrate in the presence of alternative cofactors.** *Lane 1*, substrate DNA lacking PI-*Mtu*I. The remaining lanes contained pEJ244 plasmid DNA (16 μM), PI-*Mtu*I (1 μM), and the following cofactors: 5 mM Mg^{2+} (*lane 2*); 1.5 mM ATP (*lane 3*); 5 mM Mg^{2+}-1.5 mM ATP (*lane 4*); 5 mM Mg^{2+}-1.5 mM ATPγS (*lane 5*); 5 mM Mg^{2+}-1.5 mM dATP (*lane 6*); 3 mM Mn^{2+} (*lane 7*); 3 mM Mn^{2+}-1.5 mM ATP (*lane 8*); 3 mM Mn^{2+}-1.5 mM dATP (*lane 9*); 3 mM Mn^{2+}-1.5 mM ATPγS (*lane 10*); 3 mM Zn^{2+} (*lane 11*); 3 mM Zn^{2+}-1.5 mM ATP (*lane 12*); Ca^{2+} (*lane 13*), and 3 mM Ca^{2+}-1.5 mM ATP (*lane 14*). Following incubation, reaction mixtures were deproteinized, separated on an agarose gel, and visualized as described under "Materials and Methods." The positions of substrates and products are indicated on the *left*.

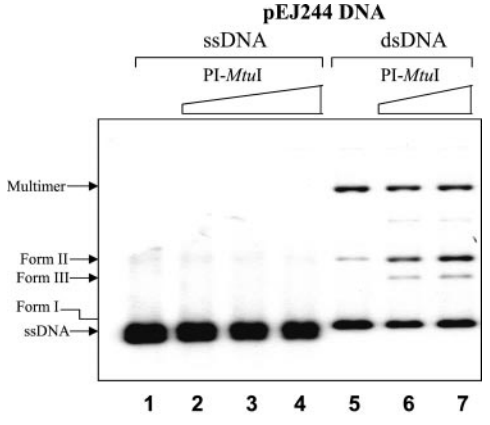

FIG. 4. **PI-*Mtu*I is a double-strand specific endonuclease.** Reaction mixtures (25 μl) containing pEJ244 DNA (16 μM) was incubated with increasing concentrations of PI-*Mtu*I in the presence of 3 mM $Mn^{2+}$and 1.5 mM ATP. Reactions were terminated and analyzed as described under "Materials and Methods." *Lanes 1* and *5*, substrate DNA lacking PI-*Mtu*I. The remaining lanes contained PI-*Mtu*I at: *lanes 2–4* at 1, 2.5, and 5 μM; *lanes 6* and *7* at 1 and 2.5 μM of PI-*Mtu*I, respectively. The positions of substrates and products are indicated on the *left*. *ssDNA*, single-stranded DNA; *dsDNA*, double-stranded DNA.

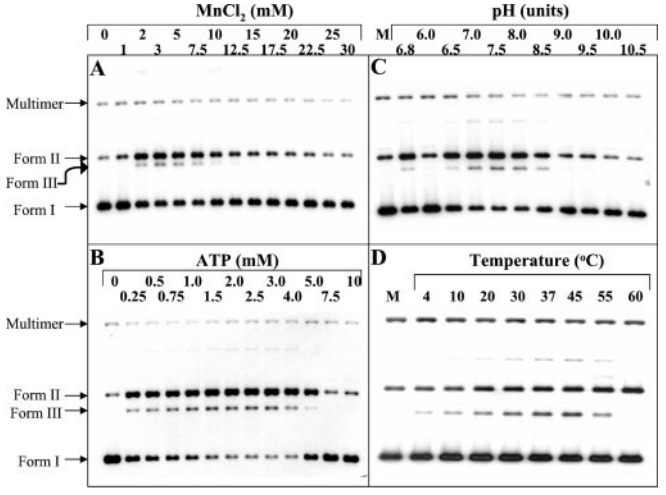

FIG. 5. **Characterization of double-stranded DNA endonuclease activity of PI-*Mtu*I.** Reactions were performed in an assay buffer (25 μl) containing 16 μM pEJ244 DNA, 1 μM PI-*Mtu*I plus the indicated treatments. *A*, reaction mixtures contained 1.5 mM ATP plus Mn^{2+} at concentrations as indicated *above each lane*. *B*, reaction mixtures contained 3 mM Mn^{2+} plus ATP at concentrations as indicated *above each lane*. *C*, reaction mixtures contained 1.5 mM ATP and 3 mM Mn^{2+} in a buffer of pH as indicated above each lane. *D*, reaction mixtures containing 1.5 mM ATP and 3 mM Mn^{2+} and were incubated at the temperature as indicated above each lane. In *C* and *D*, *lane M* represents markers. The positions of substrates and products are indicated on the *left*.

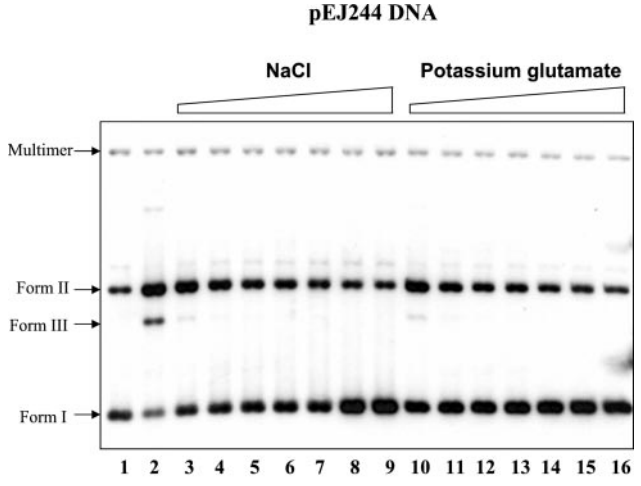

FIG. 6. **Effect of NaCl or potassium glutamate on the endonuclease activity of PI-*Mtu*I.** Reactions were performed as described in the legend to Fig. 5. *Lane 1*, substrate DNA lacking PI-*Mtu*I; *lane 2*, complete reaction. The remaining lanes contained complete reaction mixture plus NaCl (*lanes 3–9*) or potassium glutamate (*lanes 10–16*) at 50, 100, 150, 200, 300, 400, and 500 mM, respectively.

wished to investigate the kinetics and reaction pathway of PI-*Mtu*I. Given a covalently closed circular DNA containing the cleavage site, PI-*Mtu*I can cleave the substrate by two alternative mechanisms: generate linear double-stranded DNA sequentially by nicking one strand of form I DNA, followed by cutting in the second strand. Alternatively, convert supercoiled DNA directly to its linear form by cutting both the strands in a concerted manner. The data in Fig. 7*A* show the products of PI-*Mtu*I cleavage reaction as a function of time. Under these conditions, a relatively slow phase was observed in the first 30 min of the reaction, during which the amount of form I DNA declined with corresponding increase in the levels of form II DNA. A small amount of form III DNA was also produced before the reaction reached steady state by 3 h. Overall, the reaction yielded more of form II relative to form III DNA. The increase in the amount of form II and III DNA coincided with a corresponding decrease in the amount of form I DNA. To ana-

Downloaded from www.jbc.org by guest, on November 18, 2010

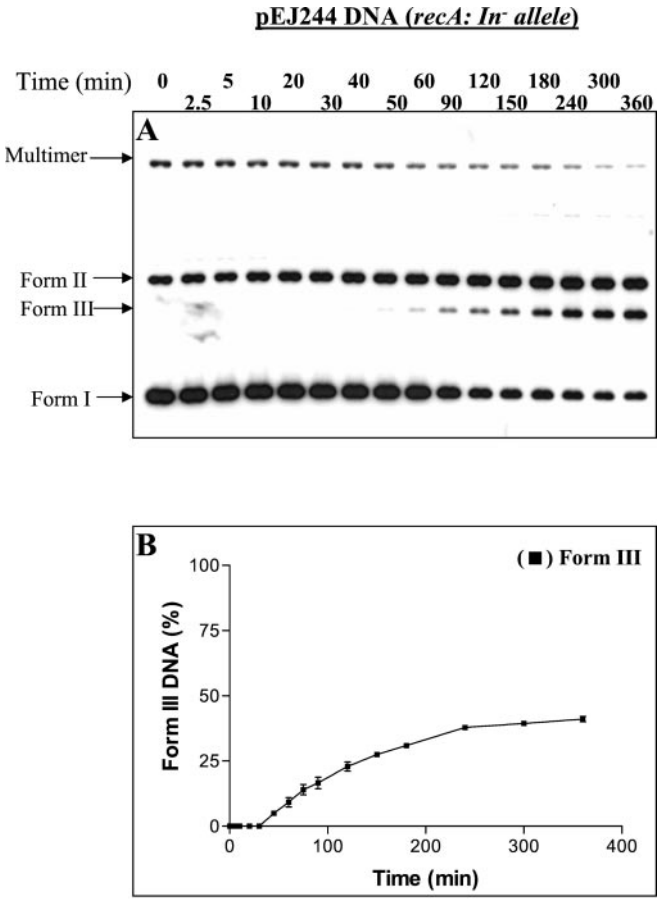

FIG. 7. **Kinetics of cleavage of target DNA by PI-*Mtu*I.** A mixture of negatively supercoiled and nicked circular duplex was incubated with PI-*Mtu*I in a standard assay buffer containing 16 μM pEJ244 DNA, 1 μM PI-*Mtu*I, 3 mM Mn^{2+}, and 1.5 mM ATP. *A*, aliquots were removed at the indicated time intervals, and the reaction was terminated. Following deproteinization, products were separated on an agarose gel as described in the legend to Fig. 5. The positions of substrates and products are indicated on the *left*. *B*, kinetics of accumulation of form III DNA as a function of time. The extent of formation of form III DNA is shown as the mean values from six independent experiments determined by scanning the autoradiograms with UVItech gel documentation system.

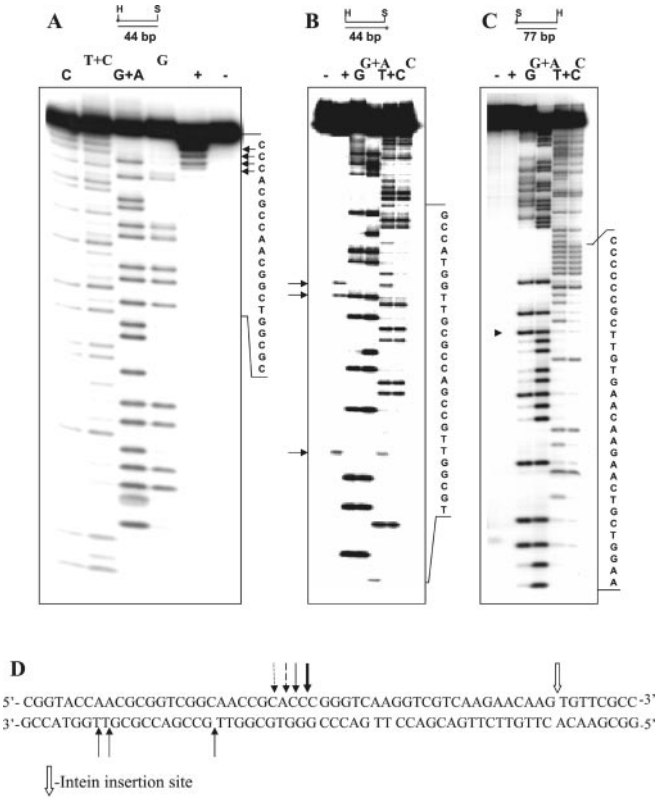

FIG. 8. **Sequence-specific cleavage of DNA by PI-*Mtu*I.** *A–C*, to determine the exact position of cleavage, DNA fragments centered surrounding the insertion site of intein-less *recA* allele were generated and individually labeled either at 3′- or 5′-end (shown as *asterisks*). The fragments were incubated either with PI-*Mtu*I or subjected to Maxam-Gilbert sequencing reaction (C, G, T+C, or G+A) as described under "Materials and Methods." The reaction mixtures were electrophoresed in a denaturing polyacrylamide sequencing gel. The + and − symbols on the *top of each panel* correspond to reactions performed in the presence or absence of PI-*Mtu*I, respectively. The nucleotide sequence surrounding the site of cleavage is shown by *horizontal arrows* on the *right side of each panel*. *D*, summary of cleavage of the target site sequence. The radioactivity in the bands at the target sequence was quantified by PhosphorImager analysis. The *open vertical arrow* denotes the site of insertion of intervening sequence in intein-less *recA* allele. *Solid* and *dotted vertical arrows* on the *upper* and *lower strands* denote the position of cleavage sites, and *thicker arrows* indicate the end result of more intense cleavage.

lyze the rate of the reaction, the percentage of product in the reaction was quantified and plotted as a function of time. Interestingly, the plot of product accumulation shows a considerable lag followed by linear increase, and then plateaus after 250 min (Fig. 7*B*). The physiological relevance of lag in product accumulation is unclear and remains to be investigated. These results, taken together with the data from Figs. 5 and 6, argue that the reaction mechanism of cleavage of target DNA by PI-*Mtu*I follows a sequential pathway. Although this mechanism is not unique, it is one of the simplest mechanisms that can fit the data presented in this report.

In regard to the slow rate of catalysis, we considered two possibilities: first, the formation of enzyme·substrate complex or the release of product from the enzyme, likely to be the rate-limiting step. In an effort to gain insights into these possibilities, we measured the rate of formation of the PI-*Mtu*I·DNA complex by SPR spectroscopy. The association rate constant (k_{on}) was in the range of 10^4 to 10^5 M^{-1} s^{-1} indicating that the formation of enzyme·DNA complex with both single- as well as double-stranded DNA was rapid (Table I). Alternatively, the overall catalytic rates may likely to be affected by the release of the product from the enzyme. A key prediction is that decrease in rate should be observed upon addition of product to an ongoing reaction. To test this possibility, kinetics of the reaction was measured in the presence of excess of product (form III DNA). Significantly, at concentrations of product from 0.05 to 1 μM, we observed no detectable inhibition in the rate of cleavage (data not shown). Second, it is possible, if not likely, that the rate of catalysis is intrinsically slow, which remains to be investigated. However, it is formally possible that the low specific activity of PI-*Mtu*I is because of the nature of the recognition site rather than the intrinsic property of the enzyme (see below).

Mapping of PI-MtuI Cleavage Sites—Cleavage sites were mapped at the nucleotide level by using ^{32}P-labeled DNA fragments produced from restriction digestion of pEJ244 plasmid DNA. The end-labeled fragments were incubated in the presence or absence of PI-*Mtu*I in standard assay buffer containing Mn^{2+}-ATP, purified on polyacrylamide gels. The cleavage products together with Maxam-Gilbert chemical sequencing ladder were separated on denaturing polyacrylamide gels (Fig. 8, *A–C*). Interestingly, all the incisions made by PI-*Mtu*I are focused in a region encompassing 22 bp around the cleavage site. On the *upper strand*, nicks were made at four contiguous positions (*lane marked* "+", Fig. 8*A*) in the left boundary 24 bp away from the site of insertion of *recA* intervening sequence

Downloaded from www.jbc.org by guest, on November 18, 2010

(*open vertical arrow* in Fig. 8*D*). Whereas on the lower strand, nicks were made at three prominent positions, a spacer of 10 bp separates the first from succeeding sites, at 34, 45, and 46 bp again in the left boundary from the place of insertion of *recA* intervening sequence (*lane marked* "+", Fig. 8*B*). Intriguingly, we found no detectable cleavage at the exact site of insertion of *recA* intervening sequence (*arrowhead* in Fig. 8*C*, *lane marked* "+"). Quantitation of signals corresponding to the cleavage sites on both the *upper* and *lower strands* is summarized in Fig. 8*D*. The cleavage pattern resulted in the generation of fragments with 3′ overhangs. The DNA ends produced by PI-*Mtu*I possessed 5′-phosphate and 3′-hydroxyl groups, because they could be labeled by polynucleotide kinase and extendable by terminal deoxynucleotidyl transferase, respectively (data not shown). While this report was under preparation, Saves *et al*. (34) reported that the recognition and cleavage sequence site of *Pps*1 intein endonuclease (designated PI-*Mga*I) of *Mycobacterium gastri* spans 22 bp, similar to PI-*Mtu*I.

DISCUSSION

In contrast to *E. coli*, the pathway of homologous genetic recombination is poorly understood in mycobacteria: however, the protein components involved are just beginning to emerge. A growing body of evidence has emphasized the complexity of this process in *M. tuberculosis* (35, 36). Thus, previous studies have highlighted the unusual structural organization of *M. tuberculosis recA* and the mechanistic aspects of homologous recombination promoted by its gene product (6–10). Here, we report that *recA* intervening sequence encodes a novel Mn^{2+}-ATP-dependent, double-strand-specific endonuclease, which is likely to be important for homing process *in vivo*.

DNA Binding Properties of PI-MtuI—Whereas the cleavage mechanism utilized by homing endonucleases is beginning to be understood (12, 16), their interaction with DNA has remained obscure. Much of the work on DNA binding characteristics of homing endonucleases has focused on probing the interaction between the DNA sequence at the homing site and enzyme. However, there are still numerous details that we do not fully understand. Remarkably, PI-*Mtu*I bound to both single- and double-stranded DNA to somewhat similar extents in the band shift assay. More surprisingly, SPR measurements showed that PI-*Mtu*I bound both single- and double-stranded DNA with equal affinity and that the rate of association (k_{on}) was similar in magnitude. However, it was surprising to discover that binding to single-stranded DNA failed to evoke single-strand nicking activity of PI-*Mtu*I (see below). Therefore, it is possible that binding of PI-*Mtu*I to double-stranded DNA is of primary importance, whereas its binding to single-stranded DNA is ancillary.

Target Recognition by PI-MtuI—The biochemical activities associated with one or more eubacterial intein-encoded homing endonucleases are less well understood. Nevertheless, it is important to compare them with eukaryotic and archaeal homing endonucleases in regard to target site selectivity and cleavage specificity. Several studies have revealed that homing endonucleases recognize and cleave widely divergent target sites ranging from 15 to 40 bp. The long length of cleavage site is believed to confer high specificity for their target sites and avoid inadvertent cleavage of host genome (12, 15, 16). The sequence alignment of target sites of representative endonucleases from eukaryotic, eubacterial, and archaeal origin is shown in Table II. It is evident from the sequence alignment that the target sites are asymmetric in sequence and lacks a consensus motif. On the other hand, I-*Ppo*I, I-*Cre*I, and I-*Ceu*I exhibit limited symmetry near the intron insertion site (12). Interestingly, comparison of target sites revealed distinct differences in sequence as well as length. PI-*Mtu*I recognized a long target site in DNA.

TABLE II

Sequence alignment of cleavage sites of homing endonucleases

The *vertical arrows* at the *top* of the table, and in the PI-*Mtu*I column, denote intein insertion sites. The "*diamond*" symbols contiguous with the nucleotide sequence indicate the position of cleavage on the upper strand, and "*underscore*" at the lower portion of the nucleotide sequence denote the position of cleavage on the lower strand of the canonical target site. "*I-*" corresponds to intron-encoded endonuclease, and "*PI-*" corresponds to protein intein encoded endonuclease.

I-*Cre*I	GCTGGGTTCAAAACGT C_GTGA♦GACAGTTTGGT
I-*Dmo*I	AATGCCTTGCCGG_GTA A♦GTTCCGGCGCGCATG
I-*Ppo*I	GTAACTATGACTCTC_T TAA♦GGTAGCCAAATGC
I-*Sca*I	ATTGTCACATTGAGGT GCACTAGTTATTACTA
I-*Sce*I	AAGTTACGCTAGGG_AT AA♦CAGGGTAATATAGC
I-*Tev*I	CA_AC♦GCTCAGTAGATGTTTTCTTGGGT CTACCGTTTAATATTG
I-*Tev*II	TTCCAAGCTTATGAGT ATGAAGGTGAACAC_GT♦TATTC
I-*Tev*III	T♦TA_TGTATCTTTTGCGT GTACCTTTAACTTCCA
PI-*Mga*I	CGTAGCTGCCCA_GTAT♦GAG TCAGAGGTGG
PI-*Psp*I	CAAAATCCTGGCAAAC AGCTATTATGGGTATT
PI-*Sce*I	TATCTATGTCGG_GTGC♦GGAGAAAGAGGTAATG
PI-*Tli*I	GGTTCTTTATGCGG_AC AC♦TGACGGCTTTTATG
PI-*Tli*III	TAAATTGCTTGCAAAC AGCTATTACGGCTATA
PI-*Pko*I	TAGATTTTAGAT CCCTGTACCCC
PI-*Pko*II	AACAGCTACTAC GGTTACTA
PI-*Pfu*I	TACAGAAGATGGGAGGAGGGA CCGGACTCAACTTCTCAAA
PI-*Pfu*II	CGATAAGGGCAACGAATCCATGTGGAGA AGAGCCTCTATA
PI-*Tfu*I	CTTATTTAGATTTTAGGT CGCTATATCCTTCGATT
PI-*Mtu*I	AA_CGCGGTCGGCAACCGCACC♦CGGGTCACGGTCGTCAAGAACAAGTGTT

Critical insights into the molecular mechanism of DNA recognition has been inferred from the cocrystal structures of I-*Cre*I (37, 38) and I-*Ppo*I (39, 40) with their target sites, and from the apo-structures of I-*Dmo*I (41), PI-*Pfu*I (42), and PI-*Sce*I (43). Notably, sequence-specific recognition is achieved by direct intrusion of an anti-parallel β-sheet comprised of four β-strands with dimensions and curvature similar to that of the major groove. Further specificity for DNA binding is mediated by the unique pattern of hydrogen bond donors and acceptors presented by the base pairs in the major groove. However, the structures of several members of homing endonucleases must be solved with both cognate and non-cognate sites to fully understand whether all of them recognize DNA through one or more similar or totally different mechanisms.

Target Cleavage and Divalent Cation Specificity—Initially, we failed to detect endonuclease activity of PI-*Mtu*I with linear duplex DNA or oligonucleotide substrates containing the inteinless *recA* allele as substrate. This could be construed by the fact that PI-*Mtu*I inflicts a staggered double-strand break encompassing 22 bp. The lack of reports demonstrating endonuclease activity of PI-*Mtu*I, including our own previous difficulties contrasts the facile success with negatively supercoiled DNA. Perhaps this could be attributable to non-ideal behavior of PI-*Mtu*I with substrates used in previous studies.

In general, homing endonucleases show relaxed specificity in target site cleavage and often cleave variant sites as efficiently as wild-type sequences. PI-*Mtu*I cleaved target DNA less efficiently and required both Mn^{2+} and ATP. The sharing of an essential divalent cation among active sites has been a subject of fascination to the nuclease field (44). Recent studies, particularly the determination of the crystal structure of I-*Cre*I, has unveiled a novel DNA cleavage mechanism in which two catalytic active centers share three Mg^{2+} ions (37). In this regard,

Downloaded from www.jbc.org by guest, on November 18, 2010

we show that PI-*Mtu*I inflicts double-strand breaks using Mn^{2+}-ATP cofactors. We speculate that PI-*Mtu*I harbors a catalytic center with a subset of amino acid residues active in the presence of thiophilic Mn^{2+}. This is, to our knowledge, the first example of a homing endonuclease exhibiting a preference for thiophilic metal and ATP for the display of cleavage activity.

The members of the LAGLIDADG class of homing endonucleases cleave target DNA in the presence of either Mg^{2+} or Mn^{2+}, with Mg^{2+} being the preferred metal ion, and generate fragments of the same size (12, 15, 16). For example, several independent methods have demonstrated that PI-*Sce*I and PI-*Pfu*I contain two distinct active sites. This implies that the enzyme bears functionally and mechanistically different active centers for cofactors, and possibly for substrates, in the same subunit or at the interface of enzyme subunits. The strong structural conservation implies strong functional conservation. In common with a few members of the family of homing endonucleases, however, a major functional difference is in regard to NTPase properties that might be of physiological significance: PI-*Mtu*I showed a marked dependence upon ATP for cleavage of target DNA. Correspondingly, PI-*Mtu*I contains a putative ATP-binding motif (^{125}GWVGGKT^{133}) (Walker A motif) found in a wide variety of NTP, generally ATP, cleavage enzymes. The importance of ATP binding and its hydrolysis for PI-*Mtu*I cleavage remains unknown. However, as in many cases, it is possible that ATP hydrolysis might accelerate the product release after cleavage reaction by disrupting interaction between the elements of the PI-*Mtu*I·DNA complex. Alternatively, or in addition, cleavage of ATP might drive conformational transitions in PI-*Mtu*I that move appropriate domains closer or farther apart relative to each other to facilitate cleavage on both the strands. Indeed, the kinetic mechanism of the PI-*Mtu*I reaction supports a sequential rather than concerted mechanism of strand cleavage. Interestingly, the high resolution mapping of the cleavage sites in target DNA by PI-*Mtu*I revealed that cleavage sites are asymmetric in sequence.

Comparison of PI-MtuI with Other Homing Endonucleases—Homing endonucleases have been something of an enigma: The recognition and cleavage sites are exceptionally long and often asymmetric. Most of the homing endonucleases cleave their target sites adjacent to the intron or intein insertion sites to generate three to five nucleotide 3′ overhangs. Interestingly, PI-*Mtu*I cuts the canonical site in the left flanking sequence 24 bp away from the intein insertion site. Similarly, I-*Tev*I and I-*Tev*III cut at 23 and 16 bp, respectively, in the left flanking sequence away from the intron insertion site, whereas I-*Tev*II cuts at 15 bp in the right flanking sequence away from the intron insertion site. More recently, it has been demonstrated that recognition and cleavage sequence for *M. gastri Pps*1 endonuclease spans 22 bp (Table II). What would be the biological significance of inflicting breaks in the flanking sequence of the intein or intron insertion points? One obvious benefit would be to protect the integration site from exonucleolytic degradation. The additional differences between PI-*Mtu*I and other homing endonucleases presumably reflect evolutionary modifications to optimize its propagation and survival (45). Regardless of the precise mechanism, the data reported here uncover important differences between PI-*Mtu*I and the class of LAGLIDADG homing endonucleases. This study initiates further structural and functional analyses aimed at understanding the physiological role(s) of PI-*Mtu*I in *M. tuberculosis*.

Acknowledgments—We thank Drs. M. J. Colston and E. O. Davis of National Institutes for Medical Research, Mill Hill, London for plasmids.

REFERENCES

1. West, S. C. (1992) *Annu. Rev. Biochem.* **61,** 603–640
2. Kowalczykowski, S. C., Dixon, D. A., Eggleston, A. K., Lauder, S. D., and Rehrauer, W. M. (1994) *Microbiol. Rev.* **58,** 401–465
3. Kuzminov, A. (1999) *Microbiol. Mol. Biol. Rev.* **63,** 751–813
4. Cox, M. M. (1999) *Prog. Nucleic Acids Res. Mol. Biol.* **63,** 311–366
5. Roca, A. I., and Cox, M. M. (1997) *Prog. Nucleic Acids Res. Mol. Biol.* **56,** 129–223
6. Davis, E. O., Sedgwick, S. G., and Colston, M. J. (1991) *J. Bacteriol.* **173,** 5653–5662
7. Davis, E. O., Thangaraj, H. S., Brooks, P. C., and Colston, M. J. (1994) *EMBO J.* **13,** 699–703
8. Davis, E. O., Jenner, P. J., Brooks, P. C., Colston, M. J., and Sedgwick, S. G. (1992) *Cell* **71,** 201–210
9. Kumar, R. A., Vaze, M. B., Chandra, N. R., Vijayan, M., and Muniyappa, K. (1996) *Biochemistry* **35,** 1793–1803
10. Vaze, M. B., and Muniyappa, K. (1999) *Biochemistry* **38,** 3175–3186
11. Datta, S., Prabu, M. M., Vaze, M. B., Ganesh, N., Chandra, N. R., Muniyappa, K., and Vijayan, M. (2000) *Nucleic Acids Res.* **28,** 4964–4973
12. Belfort, M., and Roberts, R. J. (1997) *Nucleic Acids Res.* **25,** 3379–3388
13. Liu, X. Q. (2000) *Annu. Rev. Genet.* **34,** 61–76
14. Noren, C. J., Wang, J., and Perler, F. B. (2000) *Angew. Chem. Int. Ed. Engl.* **39,** 450–466
15. Gimble, F. S. (2000) *FEMS Microbiol. Lett.* **185,** 99–107
16. Chevalier, B. S., and Stoddard, B. L. (2001) *Nucleic Acids Res.* **29,** 3757–3774
17. Mueller, J. E., Bryk, M., Loizos, N., and Belfort, M. (1993) in *Nucleases* (Linn, S. M., Lloyd, R. S., and Roberts, R. J., eds) pp. 111–144, Cold Spring Harbor Laboratory Press, Cold Spring Harbor, NY
18. Bos, J. L., Heyting, C., Borst, P., Arnberg, A. C., and Van Bruggen, E. F. (1978) *Nature* **275,** 336–338
19. Dujon, B. (1980) *Cell* **20,** 185–197
20. Belfort, M., and Perlman, P. S. (1995) *J. Biol. Chem.* **270,** 30237–30240
21. Cole, S. T., Brosch, R., Parkhill, J., Garnier, T., Churcher, C., Harris, D., Gordon, S. V., Eiglmeier, K., Gas, S., Barry, C. E., III, Tekaia, F., Badcock, K., Basham, D., Brown, D., Chillingworth, T. *et al.* (1998) *Nature* **393,** 537–544
22. Derbyshire, V., Wood, D. W., Wu., W., Dansereau, J. T., Dalgaard, J. Z., and Belfort, M. (1997) *Proc. Natl. Acad. Sci. U. S. A.* **94,** 11466–11471
23. Mills, K. V., Lew, B. M., Jiang, S., and Paulus, H. (1998) *Proc. Natl. Acad. Sci. U. S. A.* **95,** 3543–3548
24. Shingledecker, K., Jiang, S. Q., and Paulus, H. (1998) *Gene* **207,** 187–195
25. Paulus, H. (2000) *Annu. Rev. Biochem.* **69,** 447–496
26. Cunningham, R. P., DasGupta, C., Shibata, T., and Radding, C. M. (1980) *Cell* **20,** 223–235
27. Sambrook, J., Fritsch, E. F., and Maniatis, T. (1989) *Molecular Cloning: A Laboratory Manual*, 2nd. Ed., Cold Spring Harbor Laboratory Press, Cold Spring Harbor, NY
28. Bradford, M. M. (1976) *Anal. Biochem.* **72,** 248–254
29. Laemmli, U. K. (1970) *Nature* **227,** 680–685
30. Bakshi, R. P., Galande, S., Bali, P., Dighe, R., and Muniyappa, K. (2001) *J. Mol Endocrinol.* **26,** 193–206
31. Maxam, A. M., and Gilbert, W. (1980) *Methods Enzymol.* **65,** 499–560
32. Komori, K., Ichinayagi, K., Morikawa, K., and Ishino, Y. (1999) *Nucleic Acids Res.* **27,** 4175–4182
33. Gimble, F. S., and Stephens, B. W. (1995) *J. Biol. Chem.* **270,** 5849–5856
34. Saves, I., Westrelin, F., Daffe, M., and Masson, J.-M. (2001) *Nucleic Acids Res.* **29,** 4310–4318
35. Pelicic, V., Reyrat, J.-M., and Gicquel, B. (1998) *Mol. Microbiol.* **28,** 413–420
36. Norman, E., Dellagostin, O. A., McFadden, J., and Dale, J. W. (1995) *Mol. Microbiol.* **16,** 755–760
37. Chevalier, B. S., Monnat, R. J., Jr., and Stoddard, B. L. (2001) *Nat. Struct. Biol.* **8,** 312–316
38. Heath, P. J., Stephens, K. M., Monnat, R. J., Jr., and Stoddard, B. L. (1997) *Nat. Struct. Biol.* **4,** 468–476
39. Galburt, E. A., Chevalier, B., Tang, W., Jurica, M. S., Flick, K. E., Monnat, R. J., Jr., and Stoddard, B. L. (1999) *Nat. Struct. Biol.* **6,** 1096–1099
40. Galburt, E. A., Chadsey, M. S., Jurica, M. S., Chevalier, B., Erho, D., Tang, W., Monnat, R. J., Jr., and Stoddard, B. L. (2000) *J. Mol. Biol.* **300,** 877–887
41. Silva, G. H., Dalgaard, J. Z., Belfort, M., and Van Roey, P. (1999) *J. Mol. Biol.* **286,** 1123–1136
42. Ichiyanagi, K., Ishino, Y., Ariyoshi, M., Komori, K., and Morikawa, K. (2000) *J. Mol. Biol.* **300,** 889–901
43. Duan, X., Gimble, F. S., and Quiocho, F. A. (1997) *Cell* **89,** 555–564
44. Horton, N. C., and Perona, J. J. (2001) *Nat. Struct. Biol.* **8,** 290–293
45. Lambowitz, A. M., and Belfort, M. (1993) *Annu. Rev. Biochem.* **62,** 587–622

Downloaded from www.jbc.org by guest, on November 18, 2010